SULDP-1994-5

Final State Interactions in Bose-Einstein Correlations and Source Functions

M. Biyajima, T. Mizoguchi* and G. Wilk**

Department of Physics, Faculty of Liberal Arts,

Shinshu University, Matsumoto 390, Japan

*Toba National College of Maritime Technology, Toba 517, Japan

**Soltan Institute for Nuclear Studies, Hoża 69, PL-00-681 Warsaw, Poland

August 4, 1994

Abstract

We study the Bose-Einstein correlations (BEC) with the final state interactions (FSI) based on a framework of Bowler. Several new formulae including the FSI are utilized in analyses of data for $\pi^{\pm}\pi^{\pm}$ production in e^+e^- annihilation by TPC, OPAL, DELPHI, and ALEPH Collaborations. Our results show that when the exponential and Gaussian distributions are used as the source functions the degree of coherence approaches approximately unity here. We analyse also data for $K_S^0K_S^0$ pairs at Z-pole in e^+e^- annihilation and show that within the present statistical errors there is no difference between the BEC for pions and kaons. Moreover, using the same formulae we obtain a fractional degree of coherence for the data for BEC in $p+p$ collision by NA27 Collaboration.

1 Introduction

Study of the Bose-Einstein correlations (BEC) between identical particles (bosons), i.e., the GGLP effect [1], is one of current subjects in high energy physics and heavy-ion collisions [2∼9]. In the analyses of data, the following formulae are usually used:

$$N^{(\pm\pm)}/N^{BG} = c\left[1+\lambda e^{-\beta^2 Q^2}\right](1+\gamma Q), \tag{1}$$

$$N^{(\pm\pm)}/N^{BG} = c\left[1+\lambda e^{-2\eta Q}\right](1+\gamma Q). \tag{2}$$

Here $N^{(\pm\pm)}$ and N^{BG} denote the distribution of two identical particles (positive $(++)$ and negative $(--)$ charged pairs) and the background, respectively. The fact that in source region of phase space the ratio $N^{(\pm\pm)}/N^{BG} > 1$ is named the BEC, or the GGLP effect [1∼3]. (In papers on heavy-ion collisions, it is often called the Hanbury-Brown Twiss (HBT) effect.) The β and η are parameters describing the apparent size of the source emitting particles whereas λ is usually supposed to characterize its degree of coherence (notice that for $\lambda = 1$, i.e., for purely "chaotic" source, BEC are the strongest whereas for "coherent" source i.e., for $\lambda = 0$, it vanishes [1] . Q^2 is the squared four momentum difference between two identical particles: $Q^2 = (p_1 - p_2)^2 = M_{\pi\pi}^2 - 4M_\pi^2$ for pions, and $Q^2 = M_{KK}^2 - 4M_K^2$ for kaons. It should be noticed that (1) and (2) do not contain the final state interactions (FSI). On the other hand, from theoretical studies on BEC, some authors have pointed out that the FSI [10, 13, 14], resonances effect [15, 16] and different choices of source functions [17] are important in the proper description of this ratio. By FSI we understand here (following [14]) the apparent strong repulsion between pions in isospin channel $I = 2$.

In this paper we extend the analysis of BEC with FSI performed by Bowler [14] to the new high energy e^+e^- annihilation data presented recently by TPC, OPAL, DELPHI, and ALEPH Collaborations [4∼7] and perform it also for Gaussian and Lorentzian shapes of source functions. For comparison, we have analysed also data on the BEC for $K_S^0K_S^0$ pairs at Z-pole in e^+e^- annihilation [18, 19] and data on hadron-hadron collisions by NA27 Collaboration [8]. The relevant analytic formulae with hard core $(r_0 \le r < \infty)$ for exponential and Gaussian source functions are presented in the Appendix.

2 FSI with exponential source function

To study the FSI in the BEC, Bowler [14] has proposed that the following amplitude describes the identical particle effect:

$$A_{12} = \frac{1}{\sqrt{2}} e^{i(\mathbf{p}_1+\mathbf{p}_2)\cdot\mathbf{R}} \left[\frac{(e^{2i\delta}-1)}{ikr} e^{ikr} + e^{i\mathbf{k}\cdot\mathbf{r}} + e^{-i\mathbf{k}\cdot\mathbf{r}}\right], \tag{3}$$

where $\mathbf{R} = (\mathbf{r}_1 + \mathbf{r}_2)/2$, $\mathbf{k} = (\mathbf{p}_1 - \mathbf{p}_2)/2$, and $\mathbf{r} = (\mathbf{r}_1 - \mathbf{r}_2)$. It should be noted that the rest frame of the pair is used in (3). The δ denotes the phase shift describing the FSI. For pion-pion collision the phase shift of an s-wave with $I = 2$ is taken the same as in Fig. 2 of [13], and [20], i.e., it is approximately expressed by $\delta_0^{(2)} = \frac{1}{2}a_0^{(2)}Q/(1 + 0.5Q^2)$ with $a_0^{(2)} \simeq -1.2$.

[1] In fact one should keep in mind that there are apparently also other possible factors which can cause $\lambda < 1$: One of them is the coherent property of identical bosons [11, 12].

The distribution of identical particles is obtained by taking into account of the incoherent sum of $|A_{12}|^2$:

$$N^{(\pm\pm)} = \int |A_{12}|^2 F(\mathbf{R}) F(\mathbf{r}) d^3\mathbf{r}_1 d^3\mathbf{r}_2, \tag{4}$$

where F denotes the source function which in [14] is assumed to have an exponential form:

$$F(r) = e^{-\alpha r}. \tag{5}$$

Because the function $F(\mathbf{R})$ does not contribute to the ratio in this framework, the final formula of the BEC is given by

$$N^{(\pm\pm)}/N^{BG} = 1 + \lambda \left\{ \frac{1}{(1+Q^2/\alpha^2)^2} + \frac{\sin^2\delta}{k^2} \frac{\alpha^2}{1+Q^2/\alpha^2} + 2\sin\delta\cos\delta \frac{\alpha}{k} \frac{1}{1+Q^2/\alpha^2} \right\}, \tag{6}$$

where the degree of coherence (λ) is introduced by hand, and $2k = Q$. In actual applications, we introduce the normalization factor c and correction factor $(1+\gamma Q)$ to explain the long range correlation in Q variable (cf. also (1) and (2)).

In [14], (6) was used to analyse TPC Collaboration data [4]. Here we use it also to analyse data by OPAL [5], DELPHI [6] and ALEPH [7] Collaborations and compare them with TPC data [4].[2] For the sake of comparison, we show those also the BEC without the FSI (i.e., with $\delta = 0$ in (6)):

$$N^{(\pm\pm)}/N^{BG} = c \left\{ 1 + \lambda \frac{1}{(1+Q^2/\alpha^2)^2} \right\} (1+\gamma Q). \tag{7}$$

Our results (with and without normalization factor c and correction factor γ) are shown in Table I and Fig. 1 where it is evident that when (6) is used $\lambda \to 1$. [3]

/Table I/ /Fig.1/

3 FSI with Gaussian and Lorentzian source functions

In this paragraph we calculate new formulae based on (4), assuming Gaussian and Lorentzian source functions.

3.1 Gaussian distribution: We assume the following Gaussian distribution as the source function

$$F(r) = e^{-r^2/2\beta^2}. \tag{8}$$

After some algebra and introducing the degree of coherence (λ) as Bowler, we obtain a new formula of the BEC,

$$N^{(2-)}/N^{BG} = 1 + \lambda \left\{ e^{-\beta^2 Q^2/2}\mathrm{Re}[\mathrm{erfc}(z)] + \frac{8\sin^2\delta}{\beta^2 Q^2} e^{-\beta^2 Q^2/2}\mathrm{Re}[\mathrm{erfc}(z)] + \frac{8\sin\delta\cos\delta}{\beta^2 Q^2} e^{-\beta^2 Q^2/2}\mathrm{Im}[\mathrm{erfc}(z)] \right\}, \tag{9}$$

[2] It is worthwhile to note that data by TPC, OPAL, and DELPHI Collaborations are analysed by means of Q^2 (the squared four momentum transfer), not by k^2. On the other hand, the data by ALEPH Collaboration are analysed in the rest frame of the pair. Concerning with this problem, we regard that there is no big difference between them [21].

[3] Here and below all our results were obtained by using standard CERN MINUIT program, with statistical errors. The systematic errors are not taken into account in the present analyses.

where $z = -i\beta Q/\sqrt{2}$, and

$$\mathrm{erfc}(z) = \frac{2}{\sqrt{\pi}} \int_z^{\infty} e^{-t^2} dt,$$

where we make use of the fact that

$$\mathrm{Re}[\mathrm{erfc}(-i\beta Q/\sqrt{2})] = 1. \tag{10}$$

It should be noted that for $\delta \to 0$, i.e., when the FSI is ignored,

$$N^{(\pm\pm)}/N^{BG} = c\left[1 + \lambda e^{-\beta^2 Q^2/2}\right](1 + \gamma Q). \tag{9b}$$

The difference between (1) and (9b) is attributed to the number of integrals of $N^{(\pm\pm)}$ (cf. (4)). In actual analyses, we consider two cases with and without the normalization factor c and the correction factor $(1 + \gamma Q)$.

3.2 Lorentzian distribution: Finally we assume the following power function as the source function (known as Lorentzian distribution),

$$F(r) = \frac{\eta^4}{(\eta^2 + r^2)^2}. \tag{11}$$

After the same algebra as in (9), we obtain another new formula for the BEC:

$$N^{(\pm\pm)}/N^{BG} = 1 + \lambda\left\{e^{-\eta Q} + \frac{8\sin^2\delta}{\eta^2 Q^2}(1 + \eta Q)e^{-\eta Q} + \frac{32\cos\delta\sin\delta}{Q^2}\frac{\eta}{\pi}I(Q,\eta)\right\}, \tag{12}$$

where

$$I(Q,\eta) = \int_0^{\infty} \frac{\sin(Qx)}{(x^2 + \eta^2)^2} dx.$$

Again, for $\delta \to 0$ our expression simplifies to

$$N^{(\pm\pm)}/N^{BG} = c\left[1 + \lambda e^{-\eta Q}\right](1 + \gamma Q), \tag{12b}$$

where two additional terms, c and $(1 + \gamma Q)$, are introduced as in (6). The difference between (2) and (12b) is also attributed to the number of integrals in $N^{(\pm\pm)}$.

We shall now analyse data by using (9) and (10) and regarding the scattering length $a_0^{(2)}$ as a free parameter (which, as was shown in [13], should be of the order of $-1.5 \le a_0^{(2)} \le -0.7$). Our results are shown in Table. II and Fig. 2. For the sake of comparisons, we show also results obtained from (1). As you see in Table II, the degree of coherence (λ) increases in TPC and OPAL data, as (9) is used (except for the analysis with a set of 5-parameters ($\beta, \lambda, a_0^{(2)}, \gamma$ and c) of TPC data[4]). At present it is difficult to elucidate why the degree of coherence (λ) estimated in analyses of the data by DELPHI and ALEPH Collaborations is smaller than unity. To resolve this problem, we would have to consider the background N^{BG} which depends on proper procedures utilized by various Collaborations.

In Table III we show results of analyses obtained by means of (12) and (2). It can be seen that (12) does not explain the data better than (6) and (9), moreover, it demands the values of $a_0^{(0)}$ parameter well behind the estimations provided in [13] (therefore we do not show any figures in this case).

/Tables II and III/ /Figs. 2 /

[4] Note that in this case we obtained also positive $a_0^{(2)}$, i.e., we are in fact already outside the domain of FSI which, as we said at the beginning, means in our case the repulsion between the produced bosons (pions).

4 BEC for the $K^0_S K^0_S$ pairs produced in e^+e^- annihilation

OPAL and DELPHI Collaborations reported recently [18, 19] the BEC for the $K^0_S K^0_S$ pairs at Z-pole. It allows us to study the production mechanism of the strange particle and compare the BEC for pions and kaons. The relevant phase shift of the s-wave used here [22] is shown in Fig. 3 and is fitted by the formula:

$$\delta_0^{(1)}(\mathrm{deg}) = aQ + bQ^2 + 180^0 + \sum_{i=1}^{3} c_i \left[\frac{\Gamma_i/2}{(Q-Q_i)^2 + (\Gamma_i/2)^2} - \frac{\Gamma_i/2}{(Q_i)^2 + (\Gamma_i/2)^2} \right]$$

(with $a = 16.35$, $b = 24.17$, $Q_1 = 0.630$, $\Gamma_1 = 0.071$, $c_1 = 1.07$, $Q_2 = 1.126$, $\Gamma_2 = 0.141$, $c_2 = 3.76$, $Q_3 = 1.603$, $\Gamma_3 = 0.220$ and $c_3 = 8.62$). We use this expression in (6) and (9). Our results are shown in Tables IV and V and Figs. 4 and 5. As one can see, within present errors there is no substantial difference between BEC for $K^0_S K^0_S$ pairs and pions.

/Tables IV and V/ /Figs. 3, 4 and 5/

5 Concluding remarks and discussion

Using the framework of Bowler, we have calculated FSI for Gaussian and Lorentzian source functions (cf. also Appendix) and analysed data for $\pi^\pm\pi^\pm$ production in e^+e^- annihilation by means of (9) and (12) ((6) is also used in the present analyses for comparison). We have found that the power function of Lorentzian type is not useful for the analysis of FSI.

We have found that the degree of coherence (λ) depends both on source functions and FSI and approaches approximately unity in analyses of the TPC and OPAL data by means of (9) within the statistical error. This fact could suggest that λ goes to unity in (1) when the FSI is taken into account.[5]

The data of the BEC of $K^0_S K^0_S$ pairs are also analysed by the same sets of formulae. It is found that within the present experimental errors the BEC of pions and kaons seems not to be significantly different from each other.

To look for differences between the BEC in e^+e^- annihilation and hadron-hadron collisions, we have analysed also data for $p+p$ collision at $\sqrt{s} = 400$ GeV/c by NA27 Collaboration. The results are shown in Table VI and Fig. 6. As the FSI is taken into account, the degree of coherence increases also here but only slightly and λ is always smaller than 1 (except for case of the Lorentzian source function which, however, as we have shown above, does not reproduce other data and was therefore disregarded here). Note that BEC in hadron-hadron collision seem to be different from those of e^+e^- annihilation, especially in what concerned parameter λ. The main reason is probably attributed to the leading particle effect and resonances effect in $p+p$ collision.

In the present paper we have not included the effect of resonances in the BEC. We plan to address this problem elsewhere.

/Table VI/ /Fig. 6/

[5] Another approach for the FSI, based on the paper of Suzuki[13], is given in [23]. The pure chaoticity for data of TPC Collaboration is also concluded there.

Acknowledgements: The authors would like to thank H. Aihara (TPC Collab.), S. Marcellini (OPAL Collab.), U. Amaldi, and Alessandro de Angelis (DELPHI Collab.), and T. Kageya (NA27 Collab.) for their kind correspondences about their data. Moreover, this work is partially supported by the Ministry of Education, Science and Culture (No. 06640383).

Appendix

In calculations of (6) and (9), the range of the integral is from zero to infinity. If there was a hard-core in the interaction region, we have to take into account an effective range ($r_0 \le r \le \infty$). We present two formulae with the cutoff parameter r_0.

For the exponential function, $F(r) = e^{-\alpha r}$, we have

$$\begin{aligned} N^{(\pm\pm)}/N^{BG} &= 1 + \frac{\lambda}{(\alpha r_0+1)^2+1} \\ &\cdot \left\{ \frac{\cos(Qr_0)\left[2+\alpha r_0(1+Q^2/\alpha^2)\right] + \sin(Qr_0)\left[(1-Q^2/\alpha^2)+\alpha r_0(1+Q^2/\alpha^2)\right]/(Q/\alpha)}{(1+Q^2/\alpha^2)^2} \right. \\ &\left. + \frac{2\sin^2\delta}{k^2}\frac{\alpha^2\left[\cos(Qr_0)-(Q/\alpha)\sin(Qr_0)\right]}{1+Q^2/\alpha^2} + \frac{2\sin\delta\cos\delta}{k^2}\frac{\alpha^2\left[(Q/\alpha)\cos(Qr_0)+\sin(Qr_0)\right]}{1+Q^2/\alpha^2} \right\}. \end{aligned} \tag{A1}$$

As $r_0 \to 0$, we obtain (6).

For the Gaussian distribution, $F(r) = e^{-r^2/2\beta^2}$, we have

$$\begin{aligned} N^{(\pm\pm)}/N^{BG} &= 1 + \frac{\lambda}{\sqrt{\frac{\pi}{2}}\beta^3 \mathrm{erfc}\left(\frac{r_0}{\sqrt{2}\beta}\right) + \beta^2 r_0 \exp\left(-\frac{r_0^2}{2\beta^2}\right)} \\ &\cdot \left\{ \beta^2 \mathrm{Im}\left[\frac{1}{Q}\exp\left(-\frac{r_0^2}{2\beta^2}\right)\left[\cos(Qr_0)+i\sin(Qr_0)\right] + iF_2\right] \right. \\ &\left. + \frac{2\sin^2\delta}{k^2}\mathrm{Re}(F_2) + \frac{2\sin\delta\cos\delta}{k^2}\mathrm{Im}(F_2) \right\}, \end{aligned} \tag{A2}$$

where

$$F_2 = \sqrt{\frac{\pi}{2}}\beta e^{-\beta^2 Q^2/2}\mathrm{erfc}\left(\frac{r_0}{\sqrt{2}\beta} - i\frac{\beta Q}{\sqrt{2}}\right).$$

As $r_0 \to 0$, we obtain (9).

For the power function of the Lorentzian, we have no-analytic expression.

References

[1] G. Goldhaber et al., Phys. Rev. Lett. **3** (1959) 181.

[2] B. Lörstad, Int. J. Mod. Phys. **A4** (1989) 2861.

[3] D. H. Boal, C. -K. Gelbke, and B. K. Jennings, Rev. Mod. Phys. **62**(1990) 553; see also I. V. Andreev,M. Pluemer, and R. M. Weiner, Int. J. Mod. Phys., **A8** (1993) 4577.

[4] PEP4-TPC Collab., H. Aihara et al., Phys. Rev. **D31** (1985) 996.

[5] OPAL Collab., P. D. Acton et al., Phys. Lett. **B267** (1991) 143.

[6] DELPHI Collab., P. Abreu et al., Phys. Lett. **B286** (1992) 201.

[7] ALEPH Collab., D. Decamp et al., Z. Phys. **54** (1992) 75.

[8] LEBC-EHS(NA27) Collab., M. Aguilar-Benitez et al., Z. Phys. **C54** (1992) 21.

[9] EHS/NA22 Collaboration, M. Agababyan et al., Z. Phys. **C59** (1993) 195.

[10] R. Lednicky and V. L. Lyuboshits, Sov. J. Nucl. Phys. **35** (1982) 770; see also, J. Bolz et al., Phys. Lett. **B300** (1993) 404.

[11] M. Gyulassy, S .K. Kaufmann and L. W. Wilson, Phys. Rev. **C20** (1979) 2267.

[12] M. Biyajima, Phys. Lett. **92B** (1980) 193.

[13] M. Suzuki, Phys. Rev. **D35** (1987) 3359.

[14] M. G. Bowler, Z. Phys. **C39** (1988) 81.

[15] M. G. Bowler, Z. Phys. **C46** (1990) 305.

[16] R. Lednicky and T. B. Progulova, Z. Phys. **C55** (1992) 295.

[17] R. Shimoda, M. Biyajima, and N. Suzuki, Prog. Theor. Phys. **89** (1993) 697.

[18] OPAL Collab., P. D. Acton et al., Phys. Lett. **B298** (1993) 456.

[19] DELPHI Collab., P. Abreu et al., Phys. Lett. **323** (1994) 242.

[20] N. M. Cason et al., Phys. Rev. **D28** (1983) 1586.

[21] M. G. Bowler, private communication (1993).

[22] A. Etkin et al., Phys. Rev. **D25** (1982) 1786.

[23] M. Biyajima and T. Mizoguchi, in Proceedings of the XV Inter. Warsaw Meeting on Elementary Particle Physics, eds. Z. Ajduk, S. Pokorski and A. K. Wroblewski, (1992) 474.

Table I: The data ($\pi^\pm\pi^\pm$) in e^+e^- annihilation by TPC, OPAL, DELPHI, and ALEPH Collaborations are analysed by means of (6) and (7). Several sets of parameters are used.

		α [GeV]	λ	$a_0^{(2)}$ [GeV^{-1}]	γ	c	χ^2/NDF
				$-1.5 \leq a_0^{(2)} \leq -0.7$			
TPC	eq. (6)	0.461±0.035	1.162±0.084	-0.794±0.027	—	—	42.4/36
		0.505±0.053	1.272±0.122	-0.854±0.049	—	1.024±0.021	41.0/35
		0.465±0.045	1.152±0.091	-0.700±0.778	0.041±0.018	0.953±0.014	40.7/34
	eq. (7)	0.364±0.034	0.785±0.073	—	0.128±0.034	0.830±0.031	41.4/35
OPAL	eq. (6)	0.293±0.010	1.261±0.054	-0.897±0.014	—	—	110.0/75
		0.299±0.012	1.267±0.053	-0.916±0.024	—	1.003±0.003	109.1/74
		0.302±0.017	1.273±0.059	-0.933±0.074	-0.002±0.011	1.007±0.018	109.0/73
	eq. (7)	0.209±0.008	1.012±0.065	—	0.055±0.005	0.917±0.005	146.5/74
DELPHI	eq. (6)	0.317±0.012	0.744±0.027	-0.700±0.008	—	—	125.9/74
		0.385±0.020	0.910±0.055	-0.924±0.034	—	1.026±0.005	86.5/73
		0.410±0.039	0.985±0.116	-1.018±0.119	-0.013±0.019	1.053±0.040	85.9/72
	eq. (7)	0.268±0.012	0.543±0.028	—	0.042±0.007	0.949±0.009	99.8/73
ALEPH	eq. (6)	0.359±0.013	1.091±0.037	-0.700±0.009	—	—	101.1/70
		0.389±0.022	1.175±0.069	-0.794±0.039	—	1.017±0.006	89.6/69
		0.448±0.037	1.372±0.110	-1.027±0.084	-0.049±0.022	1.118±0.051	84.0/68
	eq. (7)	0.290±0.013	0.766±0.040	—	0.050±0.010	0.928±0.013	114.5/69

Table II: The same as Table I but (9) and (1).

		β [fm]	λ	$a_0^{(2)}$ [GeV^{-1}]	γ	c	χ^2/NDF
				$-1.5 \le a_0^{(2)} \le -0.7$			
TPC	eq. (9)	0.747±0.045	1.059±0.079	-0.868±0.029	—	—	43.9/36
		0.762±0.066	1.028±0.126	-0.846±0.077	—	0.995±0.015	43.8/35
		0.796±0.055	0.934±0.073	-0.700±0.021	0.031±0.018	0.952±0.015	42.5/34
	eq. (1)	0.644±0.044	0.611±0.054	—	0.083±0.025	0.881±0.023	41.0/35
OPAL	eq. (9)	1.058±0.026	1.024±0.038	-0.962±0.018	—	—	126.7/75
		1.104±0.033	0.989±0.041	-0.893±0.036	—	0.993±0.003	119.7/74
		1.166±0.029	0.914±0.037	-0.700±0.015	0.017±0.004	0.969±0.004	113.3/73
	eq. (1)	0.946±0.025	0.713±0.036	—	0.040±0.004	0.936±0.004	118.7/74
DELPHI	eq. (9)	1.067±0.029	0.630±0.022	-0.700±0.014	—	—	110.1/74
		0.900±0.042	0.872±0.071	-1.008±0.042	—	1.017±0.004	88.6/73
		0.998±0.109	0.699±0.168	-0.760±0.303	0.018±0.014	0.987±0.022	87.1/72
	eq. (1)	0.827±0.027	0.451±0.020	—	0.033±0.007	0.963±0.008	89.1/73
ALEPH	eq. (9)	0.982±0.027	0.920±0.032	-0.700±0.012	—	—	85.8/70
		0.992±0.029	0.911±0.033	-0.700±0.012	—	1.004±0.003	84.3/69
		0.998±0.036	0.906±0.039	-0.700±0.002	-0.002±0.007	1.006±0.009	84.2/68
	eq. (1)	0.797±0.026	0.630±0.030	—	0.024±0.009	0.964±0.011	87.3/69

Table III: The same as Table I but (12) and (2).

		η [fm]	λ	$a_0^{(2)}$ [GeV^{-1}]	γ	c	χ^2/NDF
				$-1.5 \le a_0^{(2)} \le -0.7$			
TPC	eq. (12)	1.630±0.116	1.585±0.176	-1.500±0.504	—	0.952±0.007	60.2/35
		1.333±0.097	1.831±0.165	-1.500±0.733	0.112±0.031	0.849±0.027	40.7/34
	eq. (2)	0.489±0.061	1.213±0.116	—	0.133±0.040	0.826±0.037	42.3/35
OPAL	eq. (12)	2.470±0.075	2.431±0.161	-1.500±0.117	—	0.973±0.002	259.6/74
		2.115±0.068	2.287±0.133	-1.500±0.116	0.048±0.005	0.927±0.005	136.5/73
	eq. (2)	0.995±0.037	1.761±0.116	—	0.049±0.005	0.925±0.005	144.8/74
DELPHI	eq. (12)	1.950±0.071	1.184±0.069	-1.500±0.168	—	1.002±0.002	134.4/73
		1.690±0.065	1.258±0.062	-1.500±0.106	0.039±0.007	0.955±0.009	99.7/72
	eq. (2)	0.693±0.038	0.863±0.051	—	0.040±0.007	0.953±0.009	106.6/73
ALEPH	eq. (12)	1.763±0.057	1.644±0.091	-1.500±0.063	—	0.992±0.003	141.1/69
		1.583±0.058	1.770±0.089	-1.500±0.057	0.043±0.010	0.938±0.012	119.4/68
	eq. (2)	0.642±0.034	1.203±0.069	—	0.045±0.011	0.936±0.013	136.0/69

Table IV: Analyses of the data of $K_S^0 K_S^0$ pairs at Z-pole by OPAL Collaboration by means of (6)-(7), (9)-(1) and (2). The Phase shift $a_0^{(1)}$ is used by means of phenomenological fit in Fig. 3.

	α [GeV], β or η [fm]	λ	γ	c	χ^2/NDF
eq. (6)	0.265±0.073	1.240±0.608	0.260±0.247	0.727±0.194	2.8/6
eq. (7)	0.364±0.129	1.191±0.517	0.150±0.131	0.836±0.126	2.1/6
eq. (9)	0.998±0.235	0.740±0.353	0.159±0.128	0.829±0.116	2.1/6
eq. (1)	0.609±0.158	0.902±0.379	0.105±0.096	0.892±0.093	2.0/6
eq. (2)	0.496±0.219	1.784±0.789	0.147±0.145	0.840±0.144	2.2/6

Table V: The same as in Table IV but for DLEPHI Collaboration data.

	α [GeV], β or η [fm]	λ	γ	c	χ^2/NDF
eq. (6)	0.200±0.070	1.337±0.804	0.131±0.143	0.839±0.141	9.9/8
eq. (7)	0.267±0.096	1.411±0.739	0.085±0.100	0.892±0.104	9.0/8
eq. (9)	1.309±0.308	0.999±0.531	0.091±0.097	0.887±0.098	8.8/8
eq. (1)	0.839±0.206	1.224±0.590	0.052±0.078	0.935±0.083	8.5/8
eq. (2)	0.709±0.314	2.143±1.234	0.074±0.099	0.908±0.107	9.2/8

Table VI: Analyses of the data ($\pi^{\pm}\pi^{\pm}$) of $p+p$ collision by NA27 Collaboration by means of (6)-(7), (9)-(1) and (2).

	α [GeV] or β [fm]	λ	$a_0^{(2)}$ [GeV^{-1}]	γ	c	χ^2/NDF
			$-1.5 \le a_0^{(2)} \le -0.7$			
eq. (6)	0.190±0.006	0.665±0.022	-0.747±0.038	—	—	71.4/37
	0.246±0.012	0.845±0.036	-1.384±0.070	—	1.045±0.009	38.1/36
	0.221±0.009	0.729±0.025	-0.700±0.000	0.135±0.026	0.942±0.011	34.1/35
eq. (7)	0.203±0.008	0.628±0.022	—	0.223±0.034	0.884±0.015	32.0/36
eq. (9)	1.641±0.030	0.529±0.015	-0.700±0.011	—	—	68.9/37
	1.580±0.064	0.584±0.038	-0.979±0.155	—	1.011±0.005	58.5/36
	1.604±0.043	0.546±0.017	-0.700±0.009	0.038±0.018	0.987±0.008	55.8/35
eq. (1)	1.192±0.032	0.453±0.015	—	0.084±0.021	0.957±0.009	51.9/36
eq. (2)	0.818±0.052	1.032±0.043	—	0.315±0.061	0.844±0.026	27.8/36

Figure Captions

Fig. 1: (a) The data for $(\pi^{\pm}\pi^{\pm})$ production at Z-pole by OPAL Collaboration are analysed by means of (6) and (7). (b) The same as Fig. 1 (a) but for DELPHI Collaboration. Data expressed by open circles are not take into account in analyses, due to resonances. (c) The same as Fig. 1 (a) but for ALEPH Collaboration. Data are read by eye-ball.

Fig. 2: (a) The data by TPC Collaboration are analysed by means of (9) and (1). (b) The same as Fig. 2 (a) but for OPAL Collaboration. (c) The same as Fig. 2 (a) but DELPHI Collaboration. (d) The same as Fig. 2 (a) but for ALEPH Collaboration. Data are read by eye-ball.

Fig. 3: Phase shift of s-wave of $K_S^0 K_S^0$ collisions used in our calculations. The following parameters are used: $a = 16.35$, $b = 24.17$, $Q_1 = 0.630$, $\Gamma_1 = 0.071$, $c_1 = 1.07$, $Q_2 = 1.126$, $\Gamma_2 = 0.141$, $c_2 = 3.76$, $Q_3 = 1.603$, $\Gamma_3 = 0.220$, and $c_3 = 8.62$.

Fig. 4: (a) Analyses of the data of $K_S^0 K_S^0$ pairs at Z-pole by OPAL Collaboration by means of (6) and (7). (b) The same as Fig. 4 (a) but (9) and (1).

Fig. 5: The same as in Fig. 4 but for data by DELPHI Collaboration.

Fig. 6: (a) Analyses of the data of $p + p$ collision by NA27 Collaboration by means of (6) and (7). (b) The same as Fig. 6 (a) but (9) and (1).

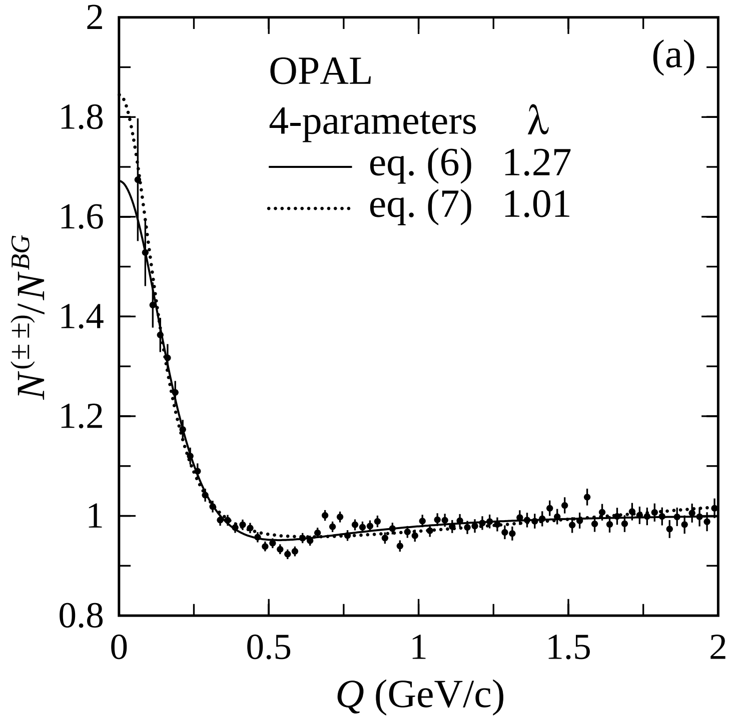
OPAL
(a)
4-parameters λ
eq. (6) 1.27
eq. (7) 1.01
$N^{(\pm\pm)}/N^{BG}$
Q (GeV/c)
0.8
1
1.2
1.4
1.6
1.8
2
0
0.5
1
1.5
2

Fig. 1

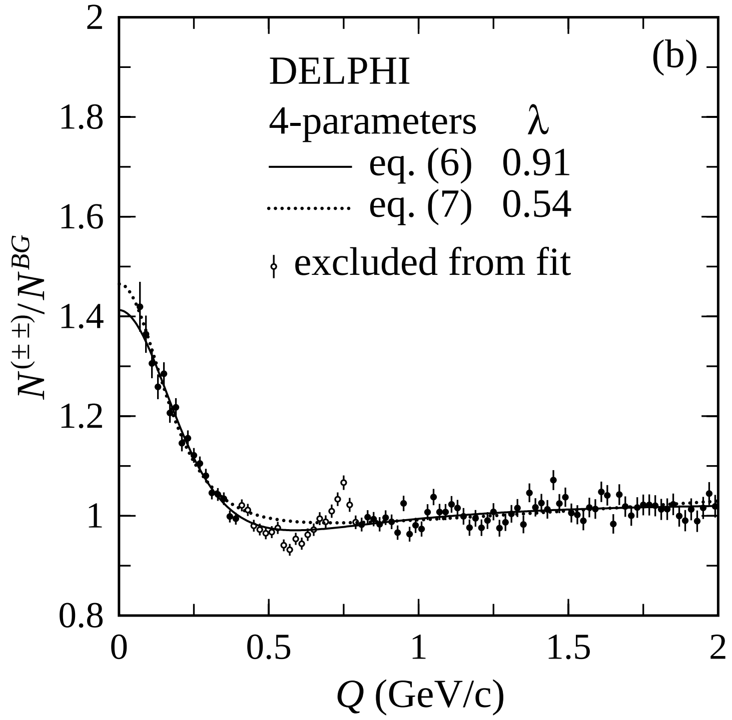
DELPHI
(b)
4-parameters λ
eq. (6) 0.91
eq. (7) 0.54
excluded from fit
$N^{(\pm\pm)}/N^{BG}$
Q (GeV/c)
0.8
1
1.2
1.4
1.6
1.8
2
0
0.5
1
1.5
2

Fig. 1

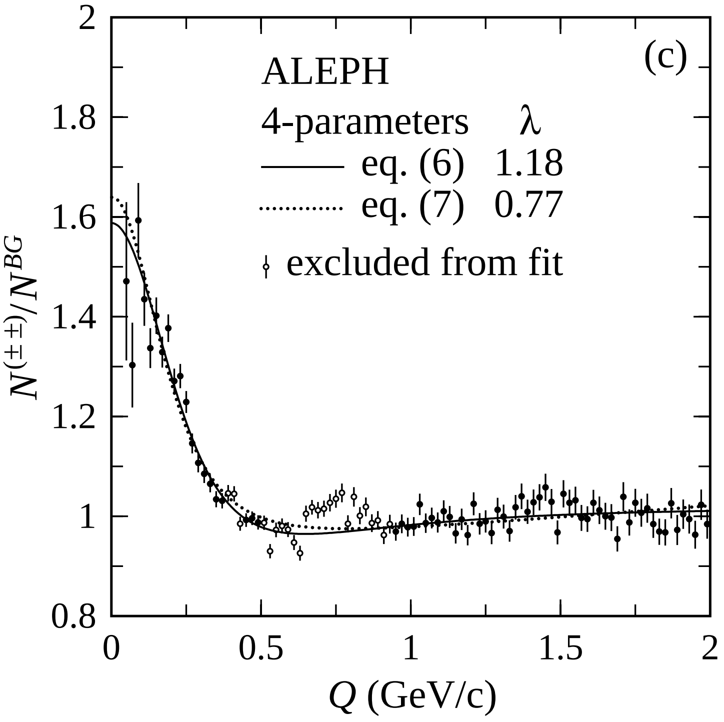
ALEPH
(c)
4-parameters λ
eq. (6) 1.18
eq. (7) 0.77
excluded from fit
$N^{(\pm\pm)}/N^{BG}$
Q (GeV/c)
2
1.8
1.6
1.4
1.2
1
0.8
0
0.5
1
1.5
2

Fig. 1

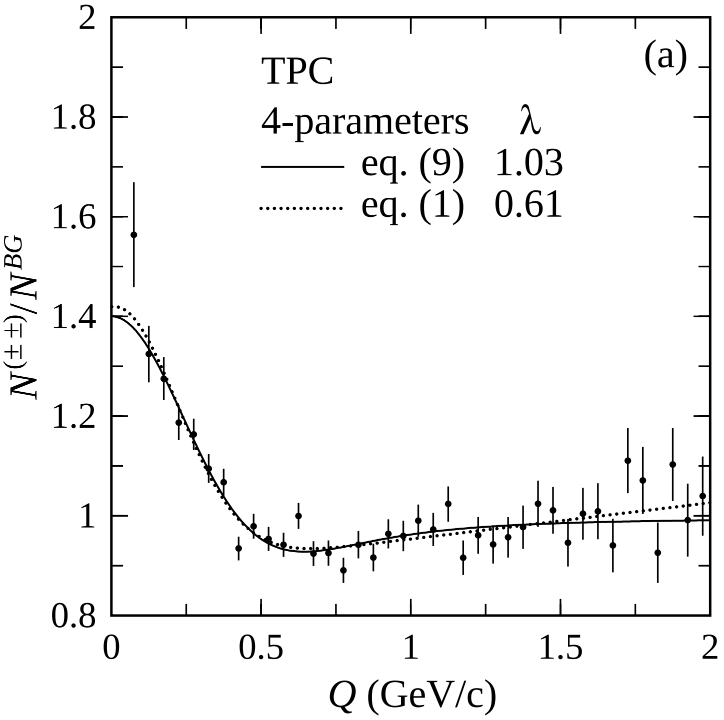
TPC
(a)
4-parameters λ
eq. (9) 1.03
eq. (1) 0.61
$N^{(\pm\pm)}/N^{BG}$
Q (GeV/c)
2
1.8
1.6
1.4
1.2
1
0.8
0
0.5
1
1.5
2

Fig. 2

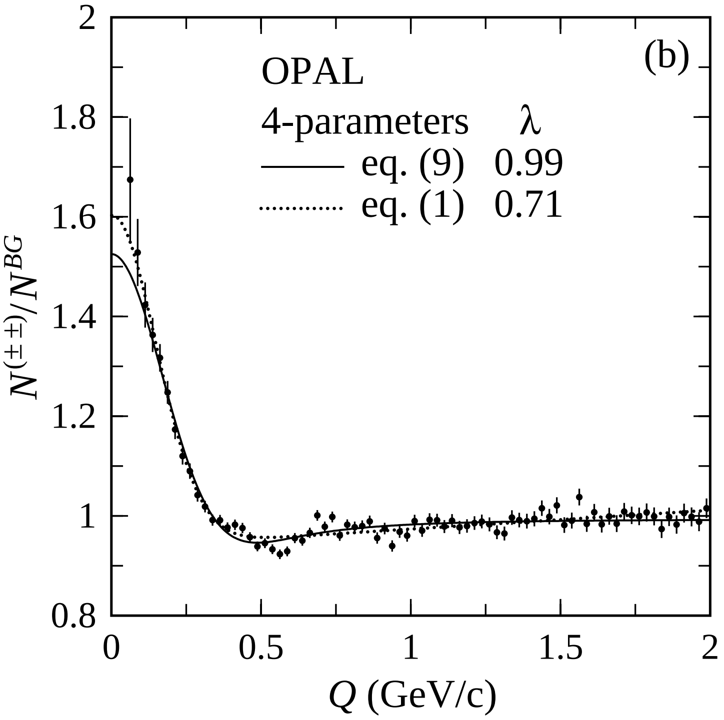

OPAL
4-parameters λ
eq. (9) 0.99
eq. (1) 0.71
(b)
$N^{(\pm\pm)}/N^{BG}$
Q (GeV/c)

Fig. 2

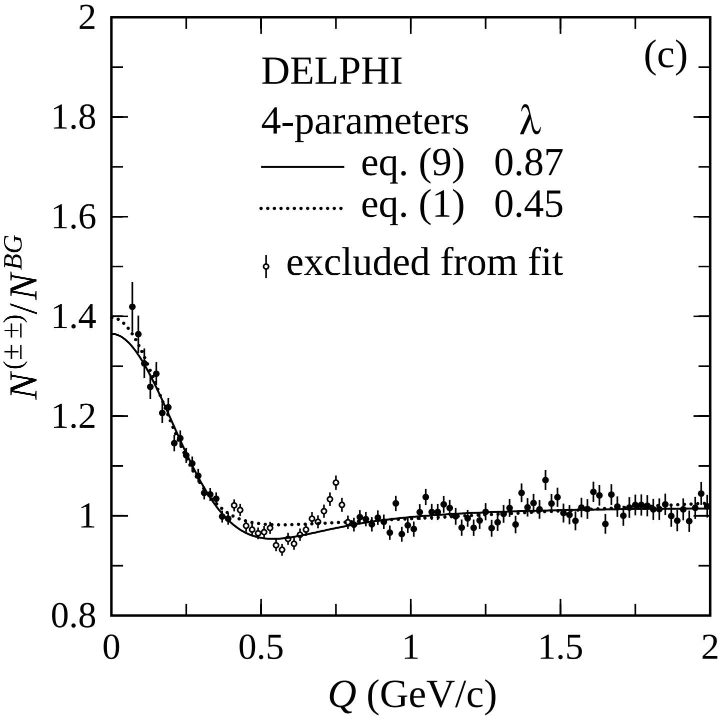

DELPHI
4-parameters λ
eq. (9) 0.87
eq. (1) 0.45
excluded from fit
(c)
$N^{(\pm\pm)}/N^{BG}$
Q (GeV/c)

Fig. 2

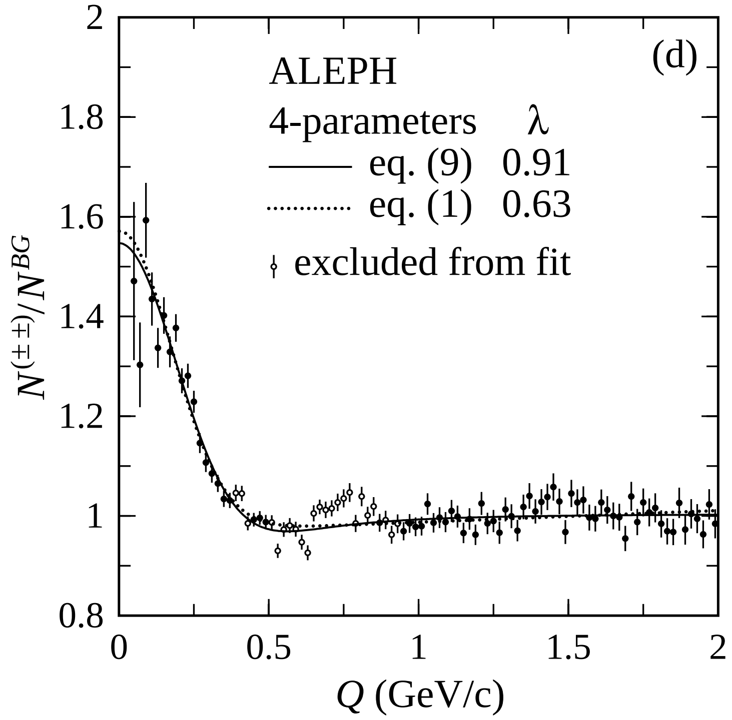

(d)
ALEPH
4-parameters λ
eq. (9) 0.91
eq. (1) 0.63
excluded from fit
$N^{(\pm\pm)}/N^{BG}$
2
1.8
1.6
1.4
1.2
1
0.8
0
0.5
1
1.5
2
Q (GeV/c)

Fig. 2

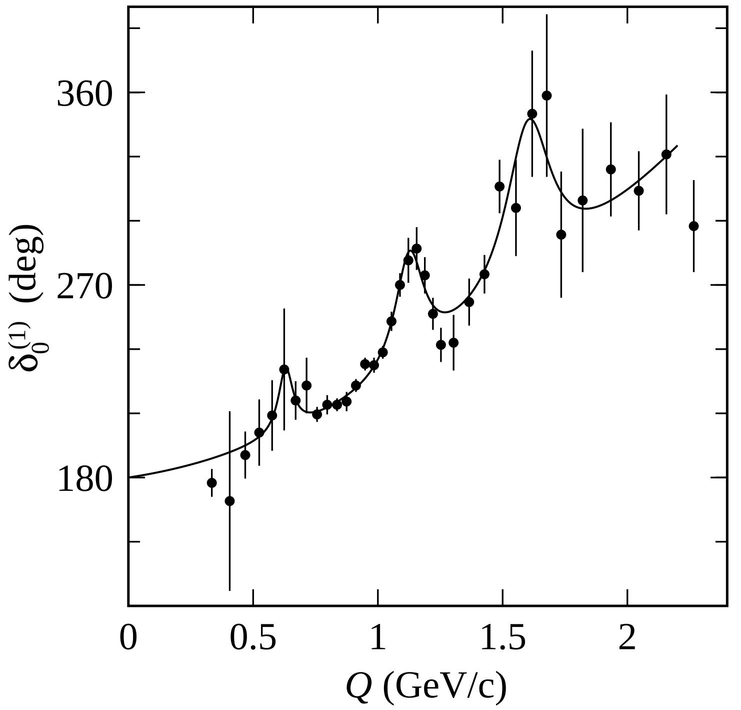

$\delta_0^{(1)}$ (deg)
360
270
180
0
0.5
1
1.5
2
Q (GeV/c)

Fig. 3

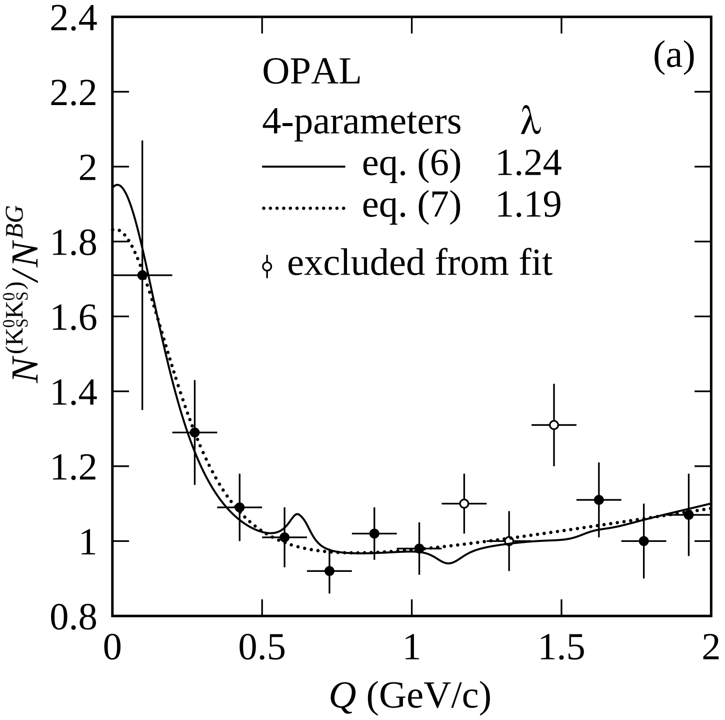
OPAL
(a)
4-parameters λ
eq. (6) 1.24
eq. (7) 1.19
excluded from fit
$N^{(K_S^0 K_S^0)}/N^{BG}$
Q (GeV/c)

Fig. 4

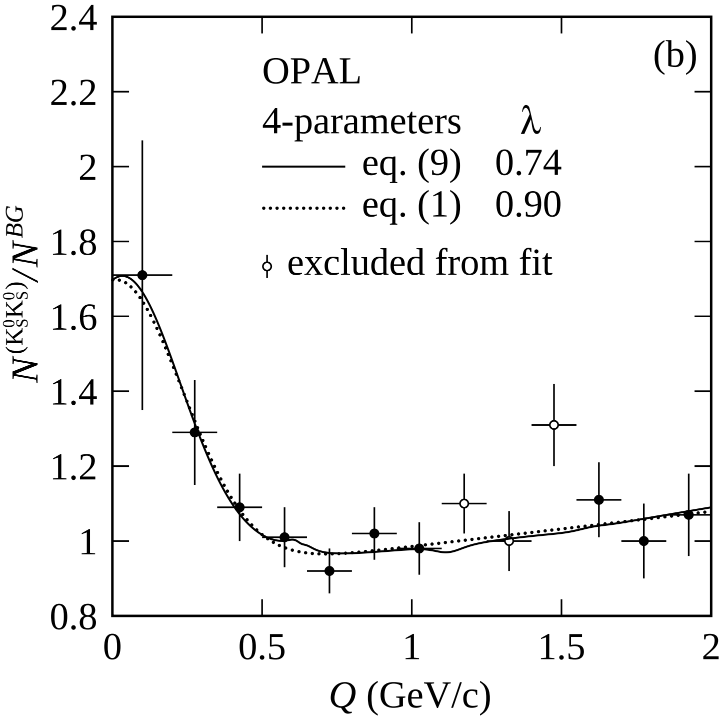
OPAL
(b)
4-parameters λ
eq. (9) 0.74
eq. (1) 0.90
excluded from fit
$N^{(K_S^0 K_S^0)}/N^{BG}$
Q (GeV/c)

Fig. 4

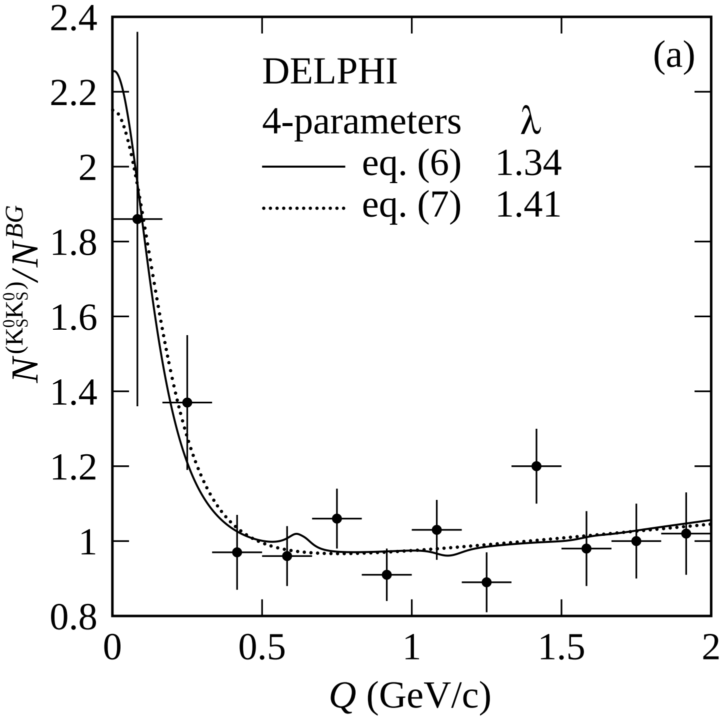
(a)
DELPHI
4-parameters λ
eq. (6) 1.34
eq. (7) 1.41
Q (GeV/c)

Fig. 5

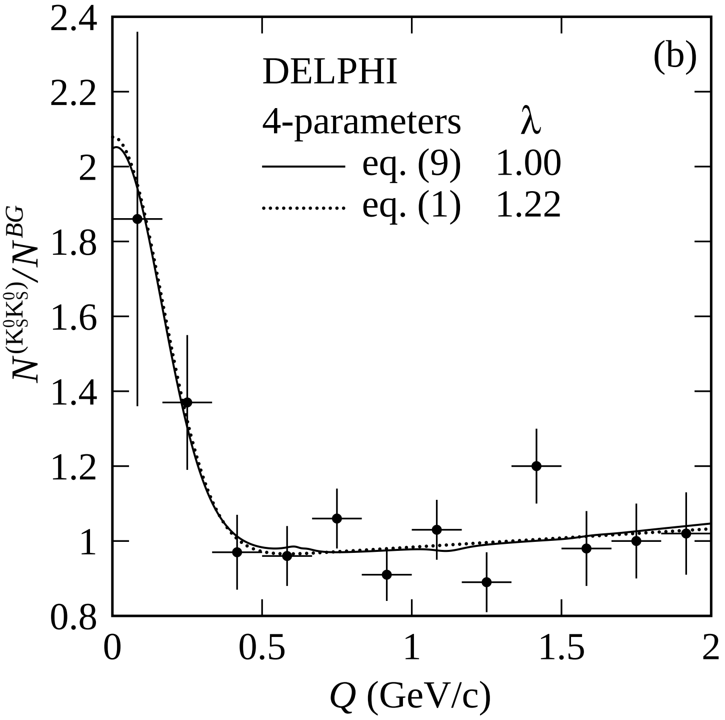
(b)
DELPHI
4-parameters λ
eq. (9) 1.00
eq. (1) 1.22
Q (GeV/c)

Fig. 5

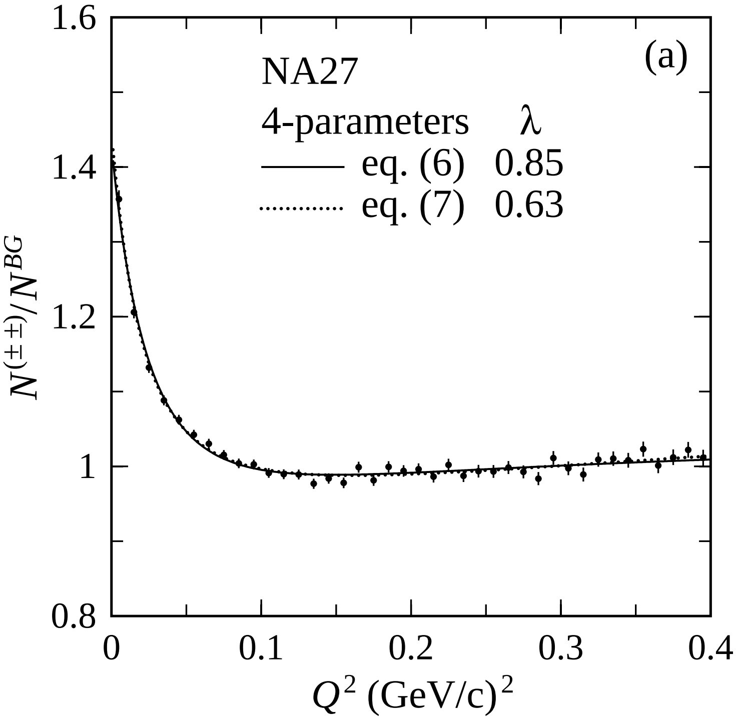

1.6
1.4
1.2
1
0.8
0
0.1
0.2
0.3
0.4
NA27
4-parameters λ
eq. (6) 0.85
eq. (7) 0.63
(a)
$N^{(\pm\pm)}/N^{BG}$
Q^2 (GeV/c)^2

Fig. 6

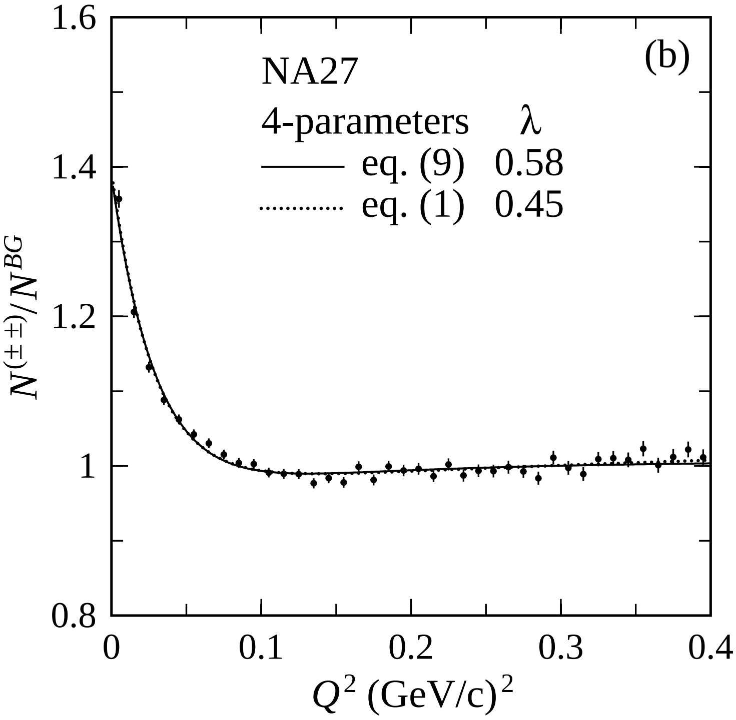

1.6
1.4
1.2
1
0.8
0
0.1
0.2
0.3
0.4
NA27
4-parameters λ
eq. (9) 0.58
eq. (1) 0.45
(b)
$N^{(\pm\pm)}/N^{BG}$
Q^2 (GeV/c)^2

Fig. 6